Development of a Minimally Invasive Robotic Interventional Radiology for Treatment of Lung Cancer

–Manufacture of a Basic Mechanism and Verification Experiment–

Takuya Inoue[1], Takayuki Matsuno[1], Akira Yanou[1], Mamoru Minami[1], Takao Hiraki[2]

[1]Graduate School of Natural Science and Technology, Okayama University, Okayama, Japan
(Tel: +81-86-251-8924; E-mail: en421807@s.okayama-u.ac.jp, {matsuno, yanou-a, minami}@cc.okayama-u.ac.jp)
[2]Okayama University Hospital, Okayama, Japan
(Tel: +81-86-235-7313; E-mail: takaoh@tc4.so-net.ne.jp)

Abstract: There are surgical methods called Interventional Radiology (IVR) using CT equipments in medical treatments of lung cancers, a blood vessels, and so on. IVR has an advantage that invasiveness is low and medical treatments with local anesthesia are possible as compare with the fact that laparotomy surgeries require general one. Therefore the number of IVR surgery has been increasing in recent years. However, radiation exposure to doctors has been concerned in the current IVR, since medical doctors conduct the treatment using CT equipment. Thus, the IVR robot should be developed in order to avoid the radioactive exposure to doctors. In this research, a robot using a parallel link mechanism is developed from the viewpoints that hand accuracy and hand rigidity are high and motors can be arranged far from CT scanning plane. The dual delta-type parallel link is proposed. It has the structure which is arranged the delta-type parallel link mechanism with three degrees of freedom (DOF). First, the arm which has offset of the axis in consideration of interference was designed. Secondly, inverse kinematics of parallel link was analyzed. Next, Delta-type parallel link mechanism with three DOF was manufactured. Finally, basic motion of parallel link robot was confirmed.

Keywords: Surgical assistant robot, less-invasive operation, Interventional Radiology

1. INTRODUCTION

In recent years, medical technology is progressing. As one of them, Interventional Radiology (IVR) is paid much attention. IVR is a surgical method which cures illness by inserting a needle or a catheter into a body while seeking its position with CT image or an ultrasonic image [1].

The appearance of IVR is shown in Fig.1. IVR is classified into two types. One is a blood circulatory system IVR, other is a non-blood one. As kinds of the blood circulatory system IVR, there are an intraarterial injection treatment and a vascular embolization. The intraarterial injection treatment is the medical procedure which injects an anticancer drug from the inside of a blood vessel to a tumor. The vascular embolization is the medical procedure which closes a blood vessel which caused bleeding or a tumor vessel. As kinds of the non-blood circulatory system IVR, there are radiofrequency ablation (RFA) and a drainage. RFA is the medical procedure which cauterizes a tumor by stabbing with a needle and generating radiofrequency waves. It is mainly used the medical treatment of lung cancer or liver cancer. The drainage is a medical procedure which excretes the pus and the blood which accumulated into the body. IVR has the advantage that invasiveness is low and the medical treatment in local anesthesia is possible as compared with the fact that a laparotomy surgery requires general one. Therefore the number of IVR surgery has been increasing in recent years.

In this paper, IVR with RFA to lung cancer is focused on. Since lungs have membrane layers including air, a cancer in lung is not reflected in a X-ray photograph and an ultrasonic image. Therefore, in IVR for lung cancer, CT equipment is widely used. In the current IVR for lung cancer, radiation exposure to medical doctors has been concerned, since doctors conduct the treatment with holding a needle beside a CT equipment.

Fig. 1 Interventional Radiology

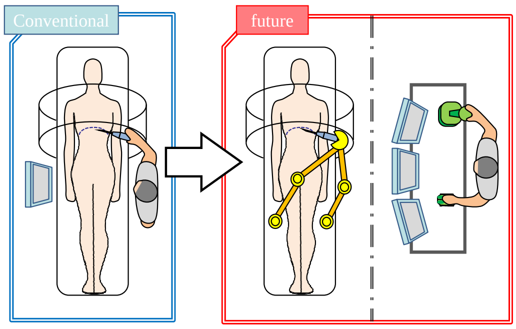

Fig. 2 Concept of Robotic IVR

Thus, radioactive exposure to medical doctors during puncture should be reduced through supporting a needle by a robot. Nowadays, some researches of surgical robots installing image guidance are studied [2],[3]. However, any surgical robots for RFA has not been developed yet. In addition, not only reduction of radioactive exposure but also reduction of the number of puncture by position control using CT image information is expectable. Our concept of Robotic IVR is shown in Fig.2. In this research, a robot which supports a needle of RFA to lung cancer is proposed.

2. ROBOTIC IVR

In this section, concept of robotic IVR is proposed. Also, specification required for robotic IVR is described.

2.1 Specification of the robot

In this subsection, specification of a robot is designed according to operation environment. Size, material, backdrivability, accuracy of position and attitude and drag of a hand are described. First, size of a robot is considered. Since IVR is conducted within the gantry of CT equipment, the robot needs to be fit into the size of inner radius of CT gantry. Next, as the phenomenon to be considered in order to realize robotic IVR, an artifact (an image which does not actually exist) which occurs on CT image is mentioned. There is a metal artifact which occurs with metal structure in an artifact through experiment. Therefore, we have to confirm how metal parts occurs artifact on CT image. Next, backdrivability is guaranteed so that a doctor can stop a robot in case of emergency and fine tune electrode needle. Backdrivability is generally higher as a gear ratio is lower. Therefore, in order to guarantee backdrivability, it is necessary to set up the gear ratio as low as possible. Next, accuracy of position and attitude of end effector is considered. The target size of the cancer which can be treated in RFA operation is from 10mm to 15mm and the range which a cancer cell becomes extinct with an electrode needle is about 20mm of proximal region of an electrode needle. Therefore, the high accuracy of puncture needle is required. With this IVR robot, the electrode needle's position accuracy of 1mm and the robot's hand position accuracy of 0.5mm are decided as target. Finally, drag of a hand considered the reactive force by puncture is required. The target drag of a hand is set to 10N based on the paper of kitamura [4].

2.2 Dual delta-type parallel link

A parallel link mechanism is adopted to IVR robot in this study. A parallel link mechanism means structure where multi links support the end effector through both of active joints and passive joints [5]. A parallel link mechanism has an advantage that hand accuracy and hand rigidity are high and a motor can be arranged far from CT scanning plane. Therefore, the occurrence of the artifact by a motor can be prevented. From viewpoints as before mentioned, the parallel link mechanism is suitable for a IVR robot.

In a joint part of the robot, the arm using the revolute joint is designed. Generally for a parallel link robot, ball joints are adopted for contraposition in passive joint. However, the ball joint has the disadvantage that a movable angle is narrow and it cannot endure high torque. On the other hand, a revolute joint generally has the disadvantage that there are many singular points. However, revolute joint has wide range of movement and is resistant to torque. For this parallel link, revolute joints are adopted from the viewpoint that range of rotation is given importance.

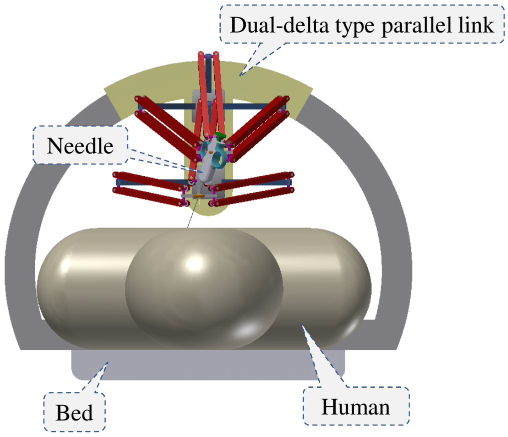

Fig. 3 Robotic IVR

In this research, the dual delta-type parallel link robot is proposed. It has the structure arranged the delta-type parallel link mechanism with three DOF as shown in Fig.3. With a delta type mechanism, an end-effector can be moved in parallel to a base platform since the axial direction of a motor and the axial direction of hand joint always keep parallel. A delta type is the typical mechanisms of a rotated type parallel link robot. One end-effector holds the upper part of a needle and the other holds the lower one. The position and attitude of a needle are controllable by controlling each end point position. Generally it will become difficult to control a robot, if robot's design-freedom increases. Since the dual delta-type parallel link robot is structure arranged the delta-type parallel link mechanism with three DOF, control is comparatively easier.

3. MODELING

In this section, modeling of a parallel link is investigated. Inverse kinematics is required to control the position of an end-effector.

3.1 Inverse kinematics

Inverse kinematics analysis of the delta-type parallel link mechanism with three DOF is conducted [5],[7]. The structure of parallel link is shown in Fig.5. The coordinates of the end-effector and the base joint B_1, B_2, B_3 are defined as (x, y, z) and $(a_1, 0, 0)$, $(0, 0, a_2)$, $(-a_3, 0, 0)$ respectively. Each angles of the base joint B_1, B_2, B_3 is defined as θ_1, θ_2, θ_3 respectively. From Fig.5, end point

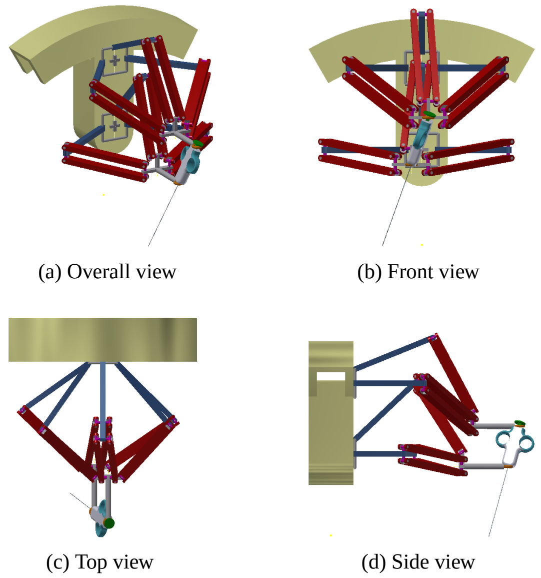

(a) Overall view (b) Front view

(c) Top view (d) Side view

Fig. 4 Dual delta-type parallel link

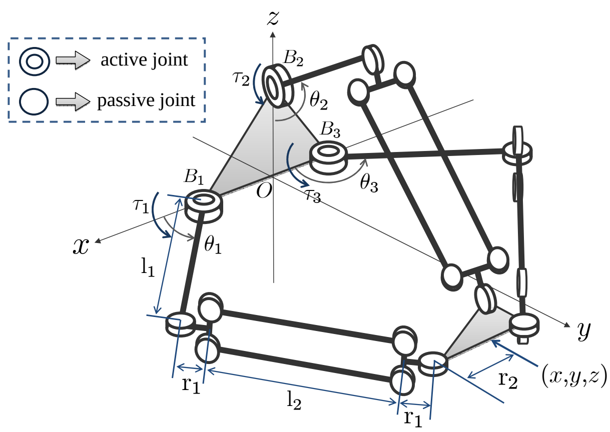

Fig. 5 Structure of parallel link

of the 1st link presented as $(a_1 + l_1 \cos\theta_1, l_1 \sin\theta_1, 0)$, $(0, l_1 \sin\theta_2, a_2 - l_1 \cos\theta_2)$, $(-a_3 + l_1 \cos\theta_3, l_1 \sin\theta_3, 0)$ respectively and end point of the 2nd link presented as $(x + r_2, y, z)$, $(x, y, z + r_2)$, $(x - r_2, y, z)$ respectively.

From geometrical condition, Eq.(1) to (3) are as follows,

$$(x + r_2 - a_1 - l_1 \cos\theta_1)^2 + (y - l_1 \sin\theta_1)^2 = \left(2r_1 + \sqrt{l_2^2 - z^2}\right)^2, \quad (1)$$

$$(z + r_2 - a_2 + l_1 \cos\theta_2)^2 + (y - l_1 \sin\theta_2)^2 = \left(2r_1 + \sqrt{l_2^2 - x^2}\right)^2, \quad (2)$$

$$(x - r_2 + a_3 - l_1 \cos\theta_3)^2 + (y - l_1 \sin\theta_3)^2 = \left(2r_1 + \sqrt{l_2^2 - z^2}\right)^2. \quad (3)$$

There are two solutions to each equations, but the 1st link must turn to the outside in order to end-effector of robot is supported. So, we can calculate θ_1, θ_2 and θ_3 as Eq.(4) to (6).

$$\theta_1 = \mathrm{atan2}\,(B_1, A_1) - \mathrm{atan2}\left(\sqrt{A_1^2 + B_1^2 - C_1^2}, C_1\right), \quad (4)$$

$$\theta_2 = \mathrm{atan2}\,(B_2, A_2) + \mathrm{atan2}\left(\sqrt{A_2^2 + B_2^2 - C_2^2}, C_2\right), \quad (5)$$

$$\theta_3 = \mathrm{atan2}\,(B_3, A_3) + \mathrm{atan2}\left(\sqrt{A_3^2 + B_3^2 - C_3^2}, C_3\right). \quad (6)$$

4. CONFIGURATION OF PROTOTYPE OF IVR ROBOT

In this research, the delta-type parallel link robot with three DOF was manufactured. The link parameters are given by Table 1. Aluminum is adopted as material of link structure in consideration of weight and intensity. The power of motor is transmitted to link though gears. Then, in the gear box, it has structure of the double-gear. Therefore, it was more compact and it became possible to increase torque of the robot. The gear ratio between a motor and the two double-gear is 6:25 and the gear ratio of the double-gear and the actuator's revolute axis is 8:25. In regard to a robot's joint portion, it is constituted by revolute joint as described in section 2. First, although the joint used revolute axis of combined unit is considered, interference with the 1st link and the 2nd link occurred. Thus, interference of links is prevented by giving offset between axis. Therefore, range of movement becomes wider. Next, arrangements of three actuators are described. Avoiding hit elbow to patient, the revolute axis of two opposite actuators turns to z axial direction. Another one turns to x axial direction. The delta-type parallel link robot with three DOF is shown in Fig.6.

Table 1 Link parameter

Symbol	Meaning	Value [mm]
a_1	Length of $\overrightarrow{OB_1}$	52
a_2	Length of $\overrightarrow{OB_2}$	81.9
a_3	Length of $\overrightarrow{OB_3}$	52
l_1	The 1st link length	150
l_2	The 2nd link length	150
r_1	Offset of 2nd link	20
r_2	Offset from end-effector to joint	44.5

5. ROBOT CONTROL

5.1 Control System

The control system of the parallel link robot is shown in Fig.7. The angle of a motor is measured by an en-

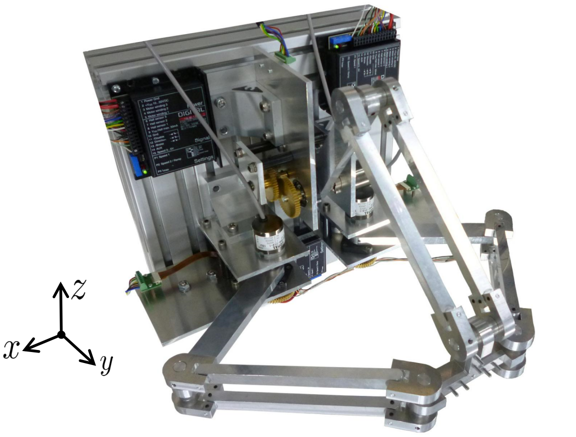

Fig. 6 Delta-type parallel link mechanism with three DOF

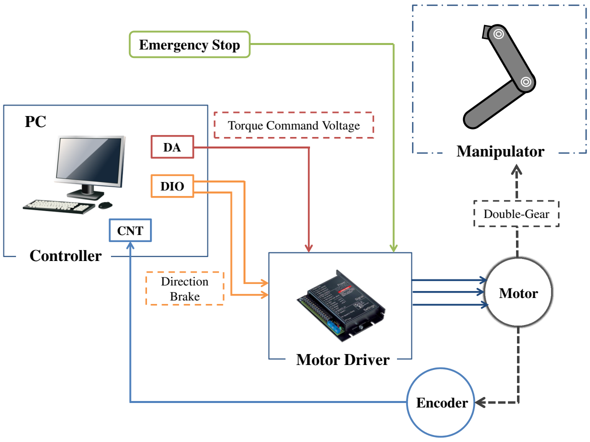

Fig. 7 Control System

coder. Based on the angle obtained, the torque of a motor and command voltage are calculated. The current, which is proportional to command voltage, is given to a motor from a motor driver. The emergency stop button is connected to motor drivers so that a robot can be stopped immediately, when the robot goes out of control. A motor is the EC flat 45 DC servo motor made by maxon, an encoder is RE30E-500-213-1, and a motor driver is motor control 1-Q-EC Amplifier DEC 50/5.

5.2 Feedback method

PID control applied gravitational compensation is used this time. The target position of a hand of a robot is represented as $\boldsymbol{p^*}$=$[x^* \ y^* \ z^*]^T$. The target angles are represented as $\boldsymbol{\theta^*}$=$[\theta^*{}_1 \ \theta^*{}_2 \ \theta^*{}_3]^T$. From inverse kinematics, the target angles of the base joint $\boldsymbol{\theta^*}$ are obtained. The angles of the base joint are represented as $\boldsymbol{\theta}$=$[\theta_1 \ \theta_2 \ \theta_3]^T$. From the above, the input torques of revolute axis $\boldsymbol{\tau}$=$[\tau_1 \ \tau_2 \ \tau_3]^T$ are calculated as follows.

$$\begin{aligned}\boldsymbol{\tau} \ &= \ \boldsymbol{k_p} \left(\boldsymbol{\theta^*}(t) - \boldsymbol{\theta}(t)\right) - \boldsymbol{k_d}\frac{d\boldsymbol{\theta}(t)}{dt} \\ &+ \ \boldsymbol{k_i} \int \left(\boldsymbol{\theta^*}(t) - \boldsymbol{\theta}(t)\right) dt + \boldsymbol{g}(\theta). \qquad (7)\end{aligned}$$

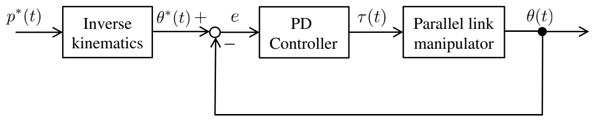

Fig. 8 Feedback control block diagram

Here, $\boldsymbol{k_p}$ is a proportional diagonal gain matrix, where k_p is each diagonal element. $\boldsymbol{k_d}$ is a derivative diagonal gain matrix, where k_d is each diagonal element. $\boldsymbol{k_i}$ is a derivative diagonal gain matrix, where k_i is each diagonal element. $\boldsymbol{g}(\theta)$ is torques for gravitational compensation. Feedback control algorithm is shown in Fig.8.

6. BASIC EXPERIMENT

The verification experiments of the hand position accuracy and backdrivability were conducted. Through the experiments, we verified below contents:

- The hand position accuracy by PD control
- The hand position accuracy applied gravitational compensation
- The hand position accuracy by PID control
- Backdrivability

The experiments were conducted under the condition where gravitational direction is oriented to negative y axis.

6.1 Verification of the hand position accuracy by PD control

First, it is verified whether end-effector could keep an initial position. Next, the desired position of end effector was moved with constant velocity and the accuracy was verified. In this experiment, PD control was adopted. An experiment procedure is as below.

1. An initial position is set up. (x=0[mm], y=270[mm], z=45[mm])
2. A hand is fixed in the state of an initial position.
3. A hand's restriction is becomes free after a certain amount of time.
4. A target position is commanded. (x^*=0[mm], y^*=220[mm], z^*=45[mm])
5. The position of a hand are varied at 30.5[mm/s] to y axis orientations.

Gain parameters k_p, k_d and k_i are set to k_p=2.0, k_d=0.2, k_i=0.0 respectively. Torques for gravitational compensation $\boldsymbol{g}(\theta)$ is not considered. The experimental results are shown in Fig.9. Angle rotation of each base joint is expressed in Fig.9(a) and joint toque of each revolute axis is expressed in Fig.9(b).

The experimental results show that the position of hand keeps stationary. However, significant errors has occurred at the initial angle. In this experiment, it is thought that such an error has occurred since effect of the weight of an arm is not taken into consideration.

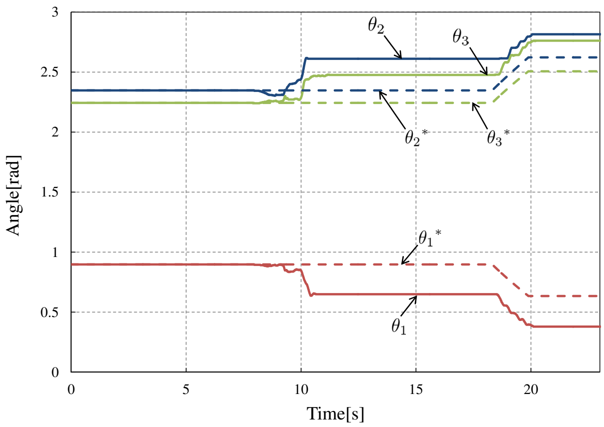

(a) Angle

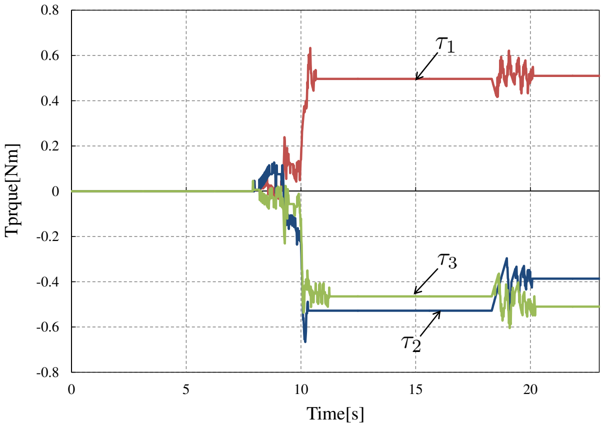

(b) Torque

Fig. 9 Experiment by PD control

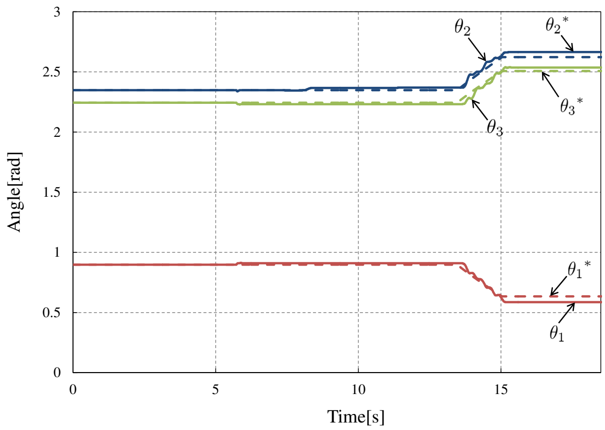

(a) Angle

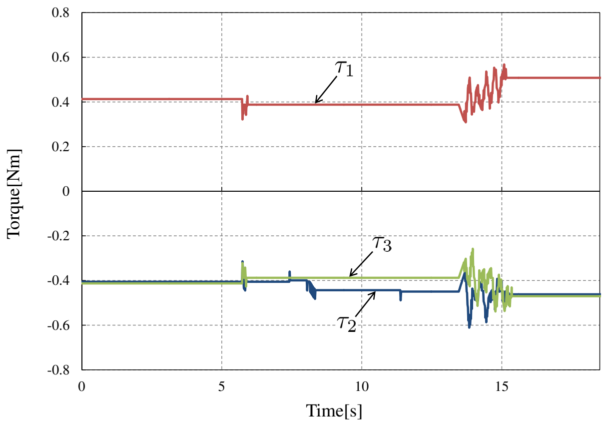

(b) Torque

Fig. 10 Experiment applied gravitational compensation

6.2 Verification of the hand position accuracy applied gravitational compensation

In order to reduce effect of arm weight, an experiment with gravitational compensation was conducted. The torque $\boldsymbol{g}(\theta)$ is adopted. The value of gain is the same as the experiment in subsection 6.1. The experimental results are shown in Fig.10. Angle rotation of each base joint is expressed in Fig.10(a) and joint toque of each revolute axis is expressed in Fig.10(b). Here, each maximum error was compared with the experiment in subsection 6.1 and they are shown in Table 2.

From the experimental result, errors become fifth times less than the result in subsection 6.1. However, errors still remain. The friction and backlash are mentioned as a factor.

6.3 Verification of the hand position accuracy by PID control

An experiment by PID control was conducted to eliminate constant errors. Integral control is introduced to the control method of subsection 6.2 and the accuracy of end-effector is verified. Gain parameters k_p, k_d and k_i are set to k_p=2.0, k_d=0.2, k_i=0.07 respectively. The experimental results are shown in Fig.11. Angle rotation of each base joint is expressed in Fig.11(a) and joint toque of each revolute axis is expressed in Fig.11(b). Furthermore, a maximum error was compared with the former experiments and it is shown in Table 2.

Table 2 Maximum errors among three experiments

Angle	PD control	applied gravitational compensation	PID control
θ_1[rad]	0.255	0.048	0.022
θ_2[rad]	0.193	0.042	0.033
θ_3[rad]	0.255	0.029	0.016

From the experimental results, maximum errors become less than half of ones in subsection 6.2. However, the end-effector has error from 1.0mm to 1.5mm. The hand accuracy of this robot falls short of criteria threshold. Furthermore, the angle did not change smoothly when the hand was moved to the target position. From the above, improvements are still required.

6.4 Verification of backdrivability

It was verified whether a end-effector could be moved by human in the state which the robot is controlled. The experimental results are shown in Fig.12. Angle rotation of each base joint is expressed in Fig.12(a) and joint toque of each revolute axis is expressed in Fig.12(b). The operator moved end-effector at about 9.0 sec and released it at about 11.0 sec.

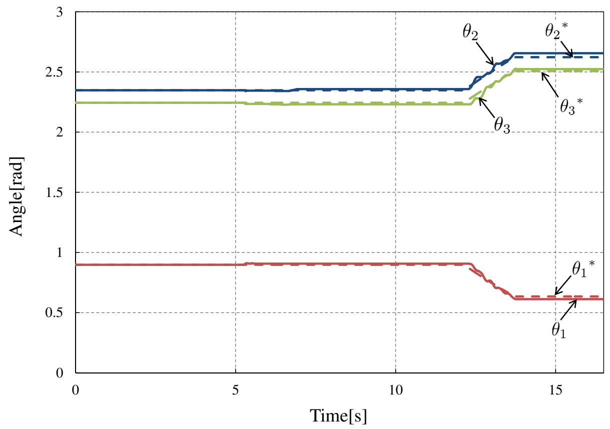

(a) Angle

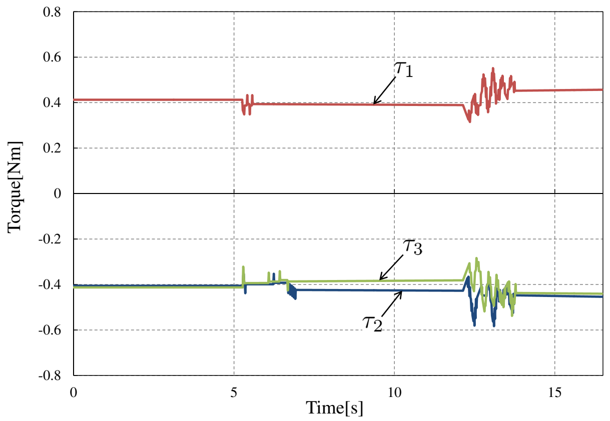

(b) Torque

Fig. 11 Experiment by PID control

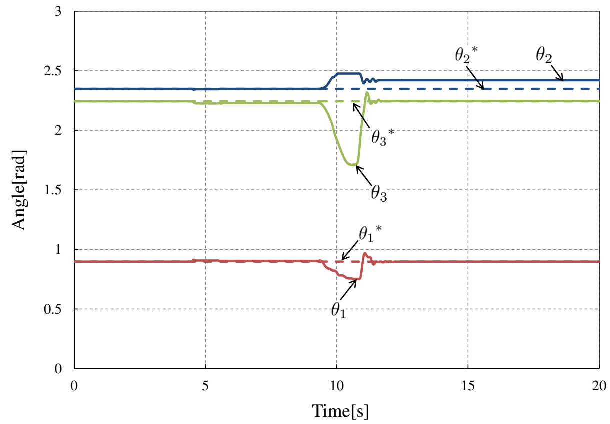

(a) Angle

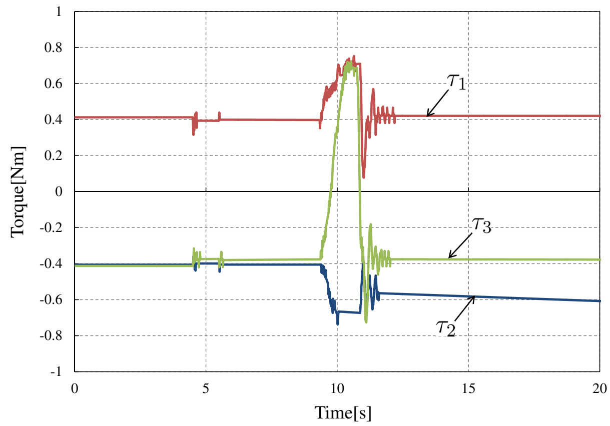

(b) Torque

Fig. 12 Verification of backdrivability

From the experiment results, it can be evaluated that this robot have comfortable backdrivability. However, θ_2 has a larger error. A shortage of torque is considered same as the experiment by PID control. From the above, low-power motor is safe for human, but is not feasible to satisfy high accuracy and backdrivability. From the viewpoint of a surgical assistant robot, accuracy should be emphasized.

7. CONCLUSION

In this paper, robotic IVR using a parallel link mechanism is proposed and the delta-type parallel link robot with three DOF was manufactured. Next, the basic experiment was conducted and confirmation of basic motion and verification of hand accuracy were conducted. In verification of hand accuracy, PD control, PD control with gravitational compensation and PID control with gravitational compensation was used and hand accuracy in each control method was confirmed. Finally, backdrivability was verified.

The torque of the motor is enlarged and it is necessary to verify hand accuracy as a future subject. In addition, the friction, backlash and accuracy of link dimensions must be considered.

REFERENCES

[1] The Japanese Society of Interventional Radiology (JSIR), " http://www.jsivr.jp/ "

[2] Daniel Glozman and Moshe Shoham, " Image-Guided Robotic Flexible Needle Steering " , IEEE TRANSACTIONS ON ROBOTICS, VOL. 23, NO. 3, pp. 459-467, 2007.

[3] Benjamin Maurin, Christophe Doignon, Jacques Gangloff, Bernard Bayle, Michel de Mathelin, Oliver Piccin, Afshin, " CTBot : A Stereotactic-Guided Robotic Assistant for Percutaneous Procedures of the Abdomen "

[4] Kitamura Hiroki, Kamegawa Tetsushi, Gofuku Akio, Hiraki Takao, " Design and development of prototypes of robotic interventional radiology " , JSME Conference on Robotics and Mechatronics, Tsukuba, Japan, May 22-25, 2013

[5] Suzumori Kouichi, " *Robot kikougaku* " [Robot kinematics], CORONA PUBLISHING CO.,LTD., 2004.

[6] Ichikawa Katsuhiro, Muramatsu Yoshihisa, " *Hyouzyun Xsen CTgazou keisoku* " [Standard X-ray CT image measurement], Ohmsha, 2009.

[7] John J. Craig, "Introduction to Robotics—mechanics and control (2nd Edition) " , Addition-Wesley, 1989.